

Preliminary Assessment of an Organic Rankine Cycle Power Plant Derived by Linear Fresnel Reflector

Elmaanaoui Youssef^{*‡}, Saifaoui Dennoun^{*}

^{*}Department of Physics, Faculty of sciences Ain Chock, University of Hassan II in Casablanca, Morocco

(elmaanaouiyoucef@gmail.com, ddsifaoui@gmail.com)

[‡]Corresponding author: Elmaanaoui Youssef, Km 8 Route d'El Jadida, B.P 5366 Maarif 20100, Casablanca 20000, Morocco, Tel: +212 618731167, elmaanaouiyoucef@gmail.com

Received: 07.08.2018 Accepted: 20.10.2018

Abstract- Organic Rankine Cycle (ORC) powered by Linear Fresnel Reflector (LFR) is a promising technology to harvest low-grade heat sources to produce electricity. This technology can be very useful especially in remote and arid areas. This work presents the study of a small-scale LFR-ORC power plant installed in Errachidia, Morocco. Simulations are conducted to evaluate the optical behaviour of the LFR based solar field and the thermal performances of the ORC based power block. Nine working fluids were tested in basic and regenerative ORCs. Results showed that the optical efficiency of the LFR changed considerably along the year and it had a great impact on the overall efficiency of the power plant. In what concerns the overall performances of the power plant, cis-butene was found to be the best choice when using a basic ORC in the power block. It allowed to achieve an annual power production of 7.12 kW with an annual overall efficiency of 5.32%. On the other hand, neopentane was found to be the best choice when using regenerative ORC in the power block. It allowed to achieve an annual power production of 7.99 kW with an annual overall efficiency of 5.97%. Regeneration enhanced the performances of the power plant by 12%.

Keywords- Organic Rankine Cycle, Linear Fresnel Reflector, working fluids, Regeneration, small-scale power plant.

Nomenclature

A_m : aperture area, m²

CSP: concentrated solar power

DVG: direct vapor generation

DNI: direct normal irradiation

GWP: global warming potential

HTF: heat transfer fluid

h : enthalpy, kJ/kg

IVG: indirect vapor generation

IAM: incidence angle modifier

IAM_{trans} : transversal incidence angle modifier

IAM_{long} : longitudinal incidence angle modifier

LFR: linear Fresnel reflector

LCOE: levelized cost of electricity

LNG: liquified natural gas

\dot{m} : mass flow rate, kg/s

NREL: national renewable energy laboratory

NIST: national institute of standards and technology

ODP: ozone depleting potential

ORC: organic Rankine cycle

PTC: parabolic trough

P_c : critical pressure, bar

\dot{Q} : heat, kJ/kg

Q_{solar} : thermal power production of the LFR, kW

s : enthalpy, kJ/kg

T : temperature, °C

T_c : critical temperature, °C

T_{cond} : condensation temperature, °C

T_{evap} : evaporation temperature, °C

TES; thermal energy storage

W_{th} : watt thermal

- W_e : watt electrical
 \dot{W} : work, kJ/kg
 η_o : reference optical efficiency
 $\eta_{s,t}$: isentropic efficiency of the turbine
 $\eta_{s,p}$: isentropic efficiency of the pump
 η_{th} : thermal efficiency of the ORC

1. Introduction

Modern life style, as we know it, relies on the continuous use of electricity. This use is unceasingly increasing especially with the rise of new economic powers such as China, India and others. And with fossil fuels being the main source of electricity worldwide, a lot of damage has been caused to the environment. To overcome this problem, several solutions have been proposed like the use of more efficient systems, the shift toward renewables, the use of smart grids and much more. One of the solutions that attracted much attention recently is the exploitation of low-grade heat sources such as geothermal, biomass, waste heat recovery and small-scale solar applications. However, in the case of low-grade heat sources, using conventional steam turbines to produce electricity is not suitable. Instead, Organic Rankine cycle (ORC) is usually proposed as an alternative and it is considered a promising technology to harness low-grade heat sources [1, 4]. From a thermodynamic point of view, ORC is the same thing as classic steam Rankine cycle and has the same thermodynamic diagram (see figure 1). An ORC consists of four processes [5]:

- Isentropic compression of the working fluid by a pump;
- Isobaric heat addition in a heat exchanger or a boiler (thermal energy is consumed during this process);
- Isentropic expansion in a turbine or in another expansion device (mechanical energy is produced during this process);
- Isobaric heat rejection in a heat exchanger.

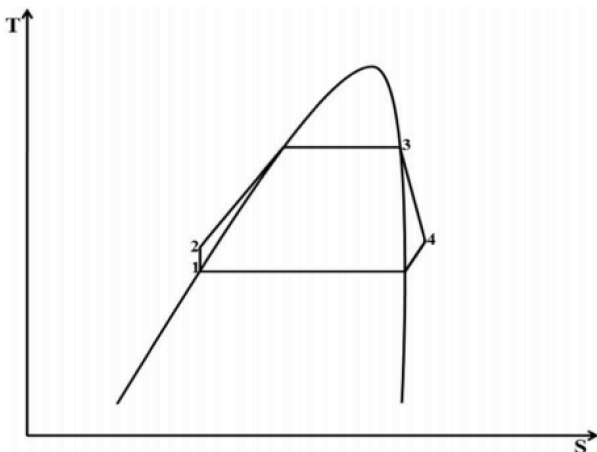


Fig. 1. the diagram of a basic ORC

The only difference between the conventional steam Rankine cycle and the ORC is the nature of the working fluid that operates the cycle; ORC uses an organic working fluid instead of water [6]. The organic fluid used is

typically a refrigerant, a hydrocarbon or a silicone oil [7]. Some of the working fluids used in the ORC exit the expansion device as superheated vapour. Such fluids allow the use of regeneration, which consists of adding another heat exchanger (a recuperator or a regenerator) to the basic configuration in order to use the heat of the superheated vapour at the outlet of the expansion device to preheat the working fluid before it enters the evaporator.

The ORC has been coupled to several technologies that ensure the required thermal energy to evaporate the working fluid, namely geothermal [8], biomass [9], waste heat of industrial processes [4], and solar energy [10]. Solar energy has become one of the most popular choice to be used with an ORC. In solar ORC applications, both concentrating and non-concentrating solar collectors can be used to drive the ORC unit. The choice of the appropriate solar technology to use is dictated by the range of temperature in consideration. Concentrated Solar Power (CSP) achieves higher temperatures than non-concentrating solar technologies, which allows the ORC unit to operate at higher evaporation temperatures leading to better thermal efficiencies. The main CSP technologies used to power ORCs are Parabolic Trough Collectors (PTC) and Linear Fresnel Reflectors (LFR). While PTC leads to better efficiencies and it is the most mature and the most established CSP technology [7], LFR is very promising especially when capital cost and land requirement are limited [11], [12]. Comparing the performances of these two CSP technologies is common in literature. For example, Cau and Cocco compared PTC to LFR in a 1MW_e ORC power plant using a silicone oil as working fluid and incorporating thermal energy storage (TES) [13]. The nominal optical efficiencies of the PTC and the LFR they used were 75% and 67% respectively, while the nominal efficiency of the ORC unit was 24.7%. Given these characteristics, they conducted a simulation using the weather data of Cagliari in Italy and they reported that the overall efficiency of the CSP-ORC system varied between 10.5% and 11% in the case of PTC and between 7.6% and 8.1% in the case of LFR. N. B. Desai and S. Bandyopadhyay also compared PTC to LFR in a 1MW_e ORC power plant. They tested 12 different working fluids in the ORC unit including water [14]. They found that Toluene had the best efficiencies in both cases (31.21% in the case of PTC and 28.14% in the case of LFR), while R113 had the lowest Levelized Cost Of Electricity (LCOE).

Other researchers focused, instead, on only one technology either PTC or LFR with the former one being heavily studied. However, LFR-ORC power plants have not been neglected and are subject to many published works. In what follows, we provide a quick survey of published works that investigated LFR-ORC power plants.

L. Cioccolanti et al studied a micro-combined LFR-ORC system to produce both heat and power [15]. They utilised a 240 m² LFR to power a 2kW_e/18kW_{th} regenerative ORC unit using NOVEC 649 as working fluid and Paratherm oil as HTF. The simulation they conducted showed that the system was able to work 3100 h/year

producing 5100 MWh/year. The peak monthly efficiency their system achieved was 31.8% recorded during July.

Cocco and Serra compared two-tank direct energy storage to thermocline Thermal Energy Storage (TES) in a 1MWe LFR-ORC power plant [16]. The total area of the LFR solar field they used was 1712 m² and it had a reference optical efficiency of 67%. The regenerative ORC unit used a silicone thermal oil as working fluid and it had a nominal efficiency of 24.7%. Authors reported in this work that two-tank direct energy storage achieved slightly higher specific energy production while thermocline had lower energy production.

S. Rodat et al worked on a dynamic model to optimize optical and thermal performances of a LFR-ORC power plant [17]. This plant consists of a 1000 m² LFR solar field coupled to a 50 kW_e ORC unit. Therminol 66 was chosen as an HTF while R245fa was selected as a working fluid. Reported results indicated that the relative error of the model was below 10%.

M. Cagnoli et al used the actual characteristics of a LFR-ORC power plant under construction to compare evacuated and non-evacuated single tube receiver [18]. This power plant is made up of an 11200 m² LFR solar field that has an annual optical efficiency of 51% and a 1MWe ORC unit with DelcoTerm Solar E15 as a working fluid. Their work showed a 10% increase in the thermal efficiency of the LFR when using evacuated tube.

F. A. Boyaghchi, A. Sohbato presented a LFR-ORC plant capable of producing power and Liquefied Natural Gas (LNG) [19]. For this purpose, they utilised a 12000 m² LFR solar field to power a 1.782 MW_{th} ORC unit using R227ea as working fluid. The nominal efficiency of the LFR they used was 25.82%, while the overall efficiency of the system at the design point was found to be 9.984%.

M. Petrollese et al investigated the performances of a LFR-ORC power plant under construction in Sardinia, Italy [20]. This plant comprises a 1432 m² LFR solar field with a reference optical efficiency of 64% and a 629 kW regenerative ORC unit that has a nominal efficiency of 20.3%. Authors predicted that this plant would operate for 2188 h/year producing 941 MWh/year with a mean efficiency of about 19.1%.

D. Cocco et al proposed the use of a LFR-ORC power plant to meet power and heat demand of a typical dairy factory [21]. For this reason, they proposed the use of a 900 m² LFR solar field that has a reference optical efficiency of 62% to power a 600 kW_e ORC unit that has a nominal efficiency of 20%. Their analysis showed that this LFR-ORC power plant could cover, almost, all the annual heat demand of the factory but only 50% of its electrical need.

The review of published works shows that researchers tend to focus in their works on only one part of the LFR-ORC system whether it is the LFR section, the ORC section or another part of the system. In contrast, only few

works have studied both the LFR and the ORC sections from optical and thermal perspectives.

In this work, we aim at the analysis of both the optical and the thermal performances of a small-scale LFR-ORC power plant given the meteorological data of Errachidia, Morocco. This area is a remote and rural part of Morocco situated in the middle of the desert where many villages are not connected yet to the electricity grid and where water is not easy to get. Thus, this work will be a preliminary assessment of the capability of such systems to meet part of the local demands.

2. Methodology

The power plant we are investigating in this work is made up of two sections: the solar field section and the power block section. Figure 2 presents the layout of this power plant. The solar field consists of the same LFR presented by P. Tsekouras et al in [22], while the power block consists of a basic ORC. In this ORC, nine working fluids are tested and the most appropriate ones are identified to operate a regenerative ORC. Direct Vapour Generation (DVG) is used as the coupling technique between the two sections of the power plant.

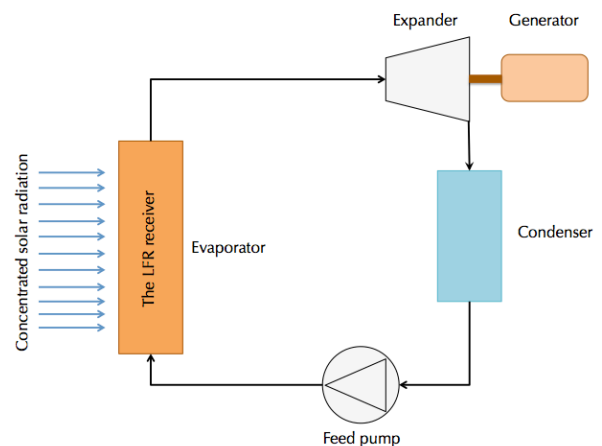


Fig. 2. Layout of the power plant investigated in this work

The performances of the power plant will be evaluated taking into consideration the geographical and meteorological data of the city of Errachidia, Morocco.

2.1. The solar field section

This work uses the same LFR system presented by P. Tsekouras et al in [22]. The schematic layout of this LFR is presented in figure 3. It consists of 16 primary reflectors, each one of them is 40 m in length and 0.3 m in width. The total width of the primary reflectors is 6.3 m, which leads to a total area of 252 m². The aperture area of the primary reflectors is 192 m² with a ground coverage of 76.2%. The receiver used is a cavity one mounted 3.5 m above the

primary reflectors. The absorber tube is installed inside the cavity and it is made of a single metallic tube of 0.14 m in diameter. Table 1 summarizes the technical characteristics of the LFR used in this study.

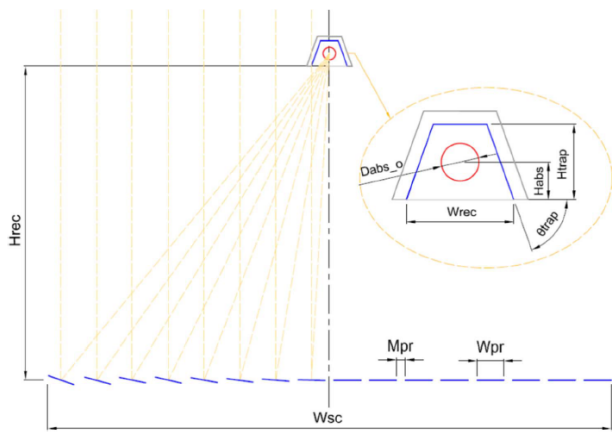


Fig. 3. A schematic layout of the LFR system presented by P. Tsekouras et al in [22]

Table 1. Characteristics of the LFR section

Number of primary reflectors	16
Gap between reflectors	0.1 m
Shape of reflectors	Slightly curved parabolic shape
Length of reflectors	40 m
Width of a reflector	0.3 m
Total solar field area	252 m ²
Aperture area of primary reflectors	192 m ²
Height of the receiver	3.5 m
Diameter of the receiver tube	0.14 m

The main objective of the LFR is to transform the solar radiation into useful thermal power. This thermal power can be calculated using equation 1.

$$Q_{solar} = DNI * \eta_0 * IAM * A_m \quad (1)$$

- DNI is the Direct Normal Irradiation available at the location where the LFR is installed;
- η_0 is the LFR's reference optical efficiency, which is the optical efficiency of the LFR at normal incidence angle;
- IAM is the Incidence Angle Modifier and it describes the variations that occur to the reference optical efficiency when sunrays are no more perpendicular to the aperture area of the LFR. IAM is a factorization of a transversal and a longitudinal components: IAM_{trans} and IAM_{long} consecutively.
- A_m is the aperture area (192 m²).

P. Tskouras et al used the Monte Carlo Ray Tracing software "SolTrace" developed by the National Renewable Energy Laboratory (NREL) Albuquerque, USA to calculate η_0 , IAM_{trans} and IAM_{long} [23]. They reported a reference optical efficiency of 69.3% and we reproduced the variation of IAM_{trans} and IAM_{long} they found in figure 4.

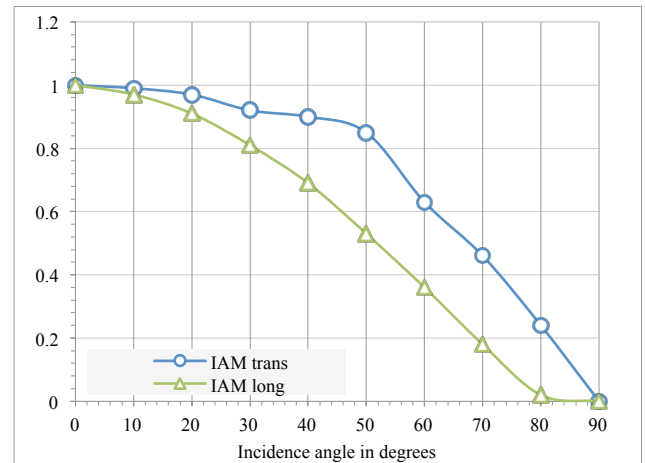


Fig. 4. variation of the transversal and the longitudinal IAM

The performances of the LFR will be evaluated through three main parameters: the optical efficiency, the operational hours and the thermal power production.

- The optical efficiency is the ratio between the solar radiation that reached the receiver and the one available at the aperture area;
- The operational hours give an idea about how long the LFR was operational during the sunshine period. In fact, even if solar radiation is available, the LFR may produce no thermal power because its optical efficiency is null. This occurs when the elevation of the sun is very low;
- The thermal power production describes the amount of heat collected by the absorber tube. This heat will serve to evaporate the working fluid.

2.2. Meteorological data

The fuel that feeds all CSP systems is the DNI. So, the determination of the available DNI resources at the location where the LFR is installed is crucial to any energy analysis of the overall system. In our case, we chose the city of Errachidia, which is located at a very arid and remote area of Morocco. In the region around this city many small villages are not connected yet to electricity grid and, thus, find very hard time to get drinking water. The DNI resources we used in this work are satellite-based data derived from the stationary satellite Meteosat. These resources and other ones can be found and downloaded from [24].

Table 2 summarizes the geographical data of the chosen location while figure 5 presents the variation of monthly DNI over the year.

Table 2. Geographical data of Errachidia, Morocco

City	Country	Latitude	Longitude	Altitude
Errachidia	Morocco	31.92°	-4.428°	1045 m

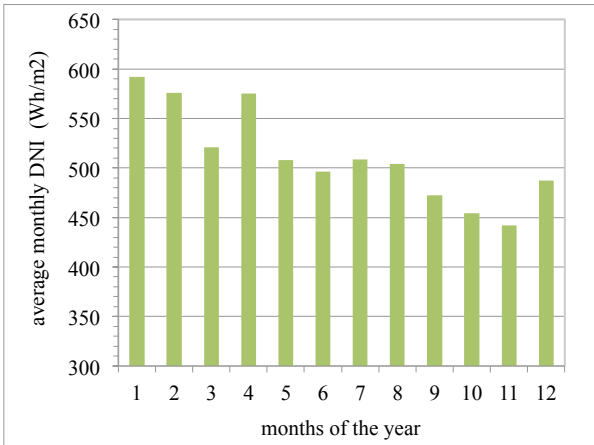


Fig. 5. available DNI resources in Errachidia, Morocco

2.3. The power block section

The power plant we are studying in this work uses a basic ORC in its power block. This basic ORC is operated between the condensation temperature of 25°C and the evaporation temperature of 150°C. The condensation

Table 3. Working fluids tested in this study

Fluid name	Type	Fluid formula	CAS N°	T _c (°C)	P _c (bar)	GWP	ODP
R123	HCFC	C ₂ HCl ₂ F ₃	306-83-2	183.68	36.618	0.02	0.02
R245ca	HFC	C ₃ H ₃ F ₅	679-86-7	174.42	39.25	720	0
R365mfc	HFC	C ₄ H ₅ F ₅	406-58-6	186.85	32.66	850	0
R245fa	HFC	C ₃ H ₃ F ₅	460-73-1	154.01	36.51	1050	0
Butane	HC	C ₄ H ₁₀	106-97-8	151.98	37.96	20	0
Cis-butene	HC	C ₄ H ₈	590-18-1	162.6	42.255	20	0
Pentane	HC	C ₅ H ₁₂	109-66-0	196.55	33.7	20	0
Neopentane	HC	C ₅ H ₁₂	463-82-1	160.59	31.96	20	0
Isopentane	HC	C ₅ H ₁₂	78-78-4	187.2	33.78	20	0

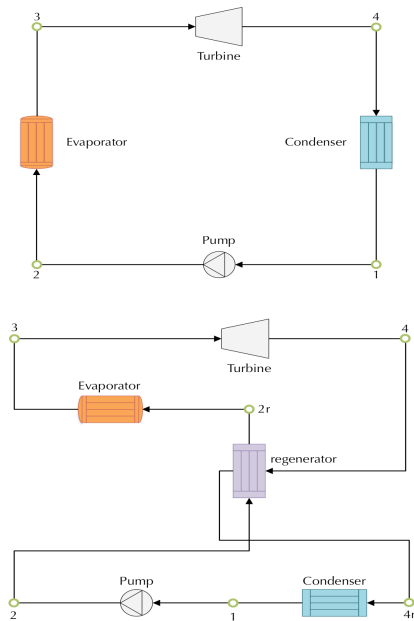


Fig. 6. layouts of the basic ORC (top) and of the regenerative ORC (down)

temperature is chosen according to the mean temperature of local water that will be used in the condenser while the evaporation temperature is used according to the range of operating temperature of the receiver provided by [22].

Nine working fluids are tested within this ORC and the most appropriate ones are selected to be tested in a regenerative ORC. The layouts of the power block in the cases of basic ORC and regenerative ORC are illustrated by figure 6. The thermodynamic properties of the selected fluids were derived from the software “REFPROP” of the National Institute of Standards and Technology (NIST), USA [25]. Table 3 presents the working fluids tested in this study giving their names, chemical formula, CAS N°, critical temperature and pressure, the Global Warming Potential (GWP) and the Ozone Depleting potential (ODP). The last two properties are environmental ones and give an idea about how much a given fluid contributes to the green house effect compared to carbon dioxide (case of GWP) and how much it contributes to depleting the ozone layer (case of ODP).

Equations used to evaluate the thermodynamic performances of each component of the power block are summarized by table 4. These equations are the same ones used by E. Ghasemian and M. A. Ehyaei in their work published in [26]. Parameters retained when carrying the simulations are given by table 5.

Table 4. equations used to evaluate the thermodynamic performances of each component

Component	Basic ORC	Regenerative ORC
The pump	$\dot{W}_{12} = \dot{m}(h_2 - h_1)$	$\dot{W}_{12} = \dot{m}(h_2 - h_1)$
The evaporator	$\dot{Q}_{23} = \dot{m}(h_3 - h_2)$	$\dot{Q}_{2r3} = \dot{m}(h_3 - h_{2r})$
The turbine	$\dot{W}_{34} = \dot{m}(h_3 - h_4)$	$\dot{W}_{34} = \dot{m}(h_3 - h_4)$
The condenser	$\dot{Q}_{41} = \dot{m}(h_4 - h_1)$	$\dot{Q}_{4r1} = \dot{m}(h_{4r} - h_1)$
The regenerator	-	$\dot{Q}_{regenerator} = \dot{m}(h_4 - h_{4r}) = \dot{m}(h_{2r} - h_2)$

In table 4, \dot{W} refers to the work produced or consumed during a given process. \dot{Q} refers to the amount of heat produced or consumed during a given process. \dot{m} is the mass flow rate of the working fluid. h is the enthalpy of the working fluid at a given state.

Table 5. parameters of the simulations

The condensation temperature	$T_{cond} = 25^{\circ}C$
The evaporation temperature	$T_{evap} = 150^{\circ}C$
The isentropic efficiency of the pump	$\eta_{s,p} = 0.7$
The isentropic efficiency of the turbine	$\eta_{s,t} = 0.7$
The temperature of the working fluid at the outlet of the regenerator	$T_{4r} = T_2 + 5^{\circ}C$

The following assumptions were made to analyse the power block section:

- All thermodynamic processes and systems are in the steady state.
- Compression and expansion of the working fluid are adiabatic.
- Pressure drops in the exchangers and piping system are neglected.

The performances of the selected working fluids and of the two configurations of the ORC are compared using the thermodynamic efficiency of the cycle, the turbine output, the condensation pressure and the evaporation pressure. Equation 2 was used to evaluate the thermodynamic efficiency of the cycle. When regenerative ORC is used, \dot{Q}_{23} is replaced by \dot{Q}_{2r3} .

$$\eta_{th} = \frac{\dot{W}_{34}}{\dot{W}_{12} + \dot{Q}_{23}} \quad (2)$$

To solve all the aforementioned equations that govern the thermodynamic behaviour of the ORC, a homemade program was elaborated by the authors using C language. This program solves the ORC using equations of table 4, simulation properties of table 5 and the thermodynamic properties of the selected working fluid (imported from REFPROP).

2.4. Validation of our model

To validate the program that we developed to carry out the simulations on the ORC, we made a comparison between results obtained using this program and those of the work of E. Georges et al published in [6]. In their work, E. Georges et al compared 6 different working fluids in a regenerative ORC operating between the temperatures of 35°C and 140°C to produce 3 kW of power. One of the working fluids they used was R123. We tested this same working fluid under the same conditions they presented in their work with the program we developed in the present work. The comparison of the obtained results is presented by table 6. A good match between our work and the work of E. Georges et al can be observed, which proves the validity of our approach.

Table 6. comparison between the present work and E. Georges et al

	Present work	E. Georges et al
Condensation pressure	1.3 bar	1.3 bar
Evaporation pressure	17.563 bar	17.6 bar
Pressure ratio	13.51	13.47
Mass flow rate	60.3 g/s	64.9 g/s
Cycle efficiency	15.3%	15%

2.5. Coupling the solar field section to the power block section

When coupling the solar field section to the power block section two configurations are possible: Indirect Vapour Generation (IVG) and Direct Vapor Generation (DVG). In the IVG configuration, an HTF collects heat from the solar field and transport it to the evaporator of the power block where the working fluid is evaporated. With this configuration, heat storage can be implemented. In the DVG, there is no HTF and the working fluid collects heat itself from the receiver of the solar field where it is directly evaporated. In this configuration, the receiver of the solar field is, in the same time, the evaporator of the power block.

This work adopts the DVG configuration for its economic advantages. In fact, using DVG results in lower capital costs since it does not use an additional fluid (the HTF) and it uses less heat exchangers (no need for the evaporator).

The overall performances of the LFR-ORC power plant are evaluated using the overall efficiency of the plant and its power production. The overall efficiency of the plant is the ratio between the power block outlet and solar radiation available at the aperture area of the LFR.

3. Results and Discussion

3.1. The solar field section

The performances of the solar field were assessed through its monthly optical efficiency, its operational hours and its thermal power production. Figures from 7 to 9 present the obtained results.

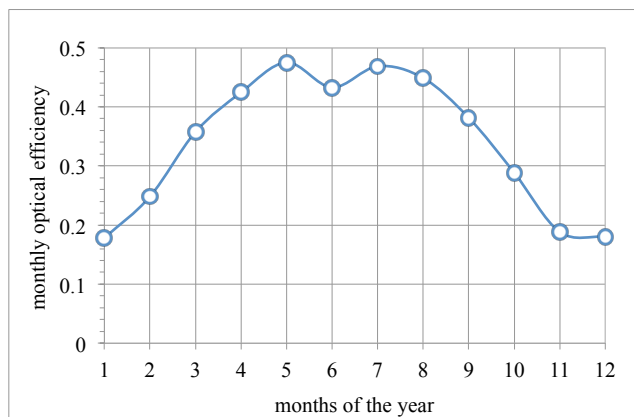


Fig. 7. Variation of the LFR’s monthly optical efficiency

Figure 7 presents the variation of the LFR’s optical efficiency on a monthly basis for the location of Errachidia. The LFR recorded the highest optical efficiency during May and it was equal 47.51%, while the lowest optical efficiency was recorded during January and it was equal 17.8%. The lowest monthly efficiency was less than half of the highest one. This shows the big variation that occurs to the optical performances of the LFR mainly due to its small size that makes it vulnerable to the changes in the solar elevation in the sky throughout the year. In addition, the optical efficiency slightly decreased during June. This same behaviour was reported by Y. Qiu et al in the work they published in [27]. However, they did not give any explanation to it. In what we concern, we think that the decrease in the LFR’s optical efficiency during June is mainly due to the increase in end losses as we demonstrated it in our work previously published in [28].

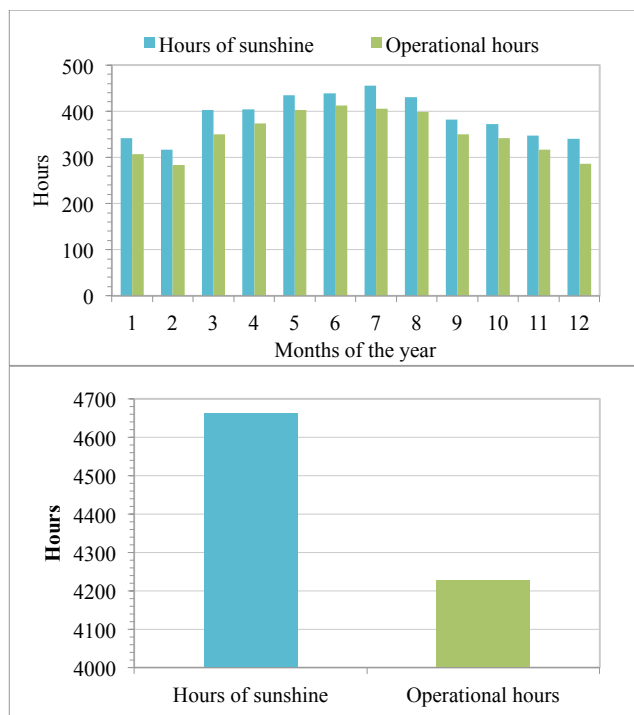


Fig. 8. Comparison of sunshine and operational hours on a monthly basis (left) and on an annual basis (right)

Figure 8 presents a comparison between sunshine hours and operational hours on a monthly and a yearly basis. Due to the optical efficiency that may be equal to zero during some periods of the day, the LFR did not benefit from all the hours of sunshine. The maximum operational hours were recorded during the month of June reaching 412 hours while the month of February was the worst one with only 283 hours. Over the whole year, the LFR was operational during 4228 hours, which represented 90.67% of the sunshine hours.

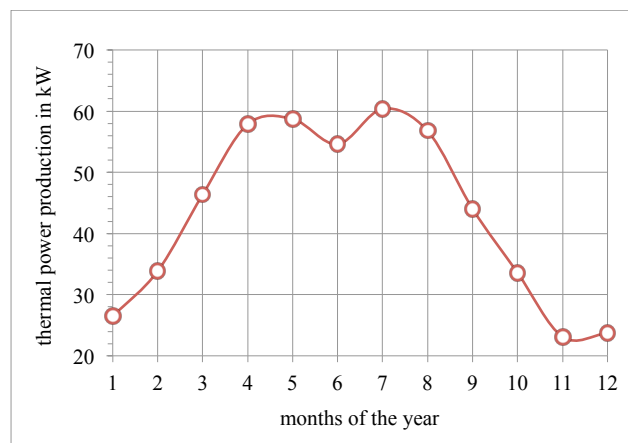


Fig. 9. Variation of monthly thermal power production of the LFR section

Figure 9 illustrates the variation of the thermal power production of the LFR during each month of the year. It shows that the thermal power production did not change significantly from April to August due to the stability of both the available solar radiation and the optical efficiency during this period. The highest thermal power production was recorded during July and it was equal to 60.4 kW, while the lowest one was recorded during November and was equal to 23.1 kW. This minimum power production represents only 38% of the maximum. Such low power production is due to the fact that during November available solar radiation is the lowest one and optical efficiency is the third lowest one.

It is worth noting that January had the highest available solar radiation but recorded the third lowest thermal power production, which shows the big impact of the optical efficiency on the LFR’s overall behaviour.

3.2. The power block section

The thermodynamic performances of the power block using the basic ORC configuration in the case of each of the nine working fluids are presented by table 7.

Table 7. The main results of the power block section in the case of the basic ORC configuration

	Evaporator pressure (bar)	Condenser pressure (bar)	Heat required (kJ/kg)	Sub-cooling heat released (kJ/kg)	Turbine output (kJ/kg)	Cycle efficiency (%)
R123	20.99	0.91	233.95	27.43	37.11	15.73
R245ca	25.58	1.01	283.46	41.75	43.23	15.11
R365mfc	16.93	0.57	302.83	64.45	44.92	14.74
R245fa	33.95	1.48	246.95	23.19	36.88	14.73
Butane	36.75	2.43	461.01	38.23	69.84	14.87
Cis-butene	34.6	2.14	490.67	27.49	78.11	15.68
Pentane	15.91	0.68	556.27	108.23	85.25	15.23
Neopentane	27	1.71	462.21	97.63	67.33	14.37
Isopentane	18.68	0.92	528.98	107.53	80.12	15.03

The thermodynamic efficiency of the power block did not change considerably when the working fluid was changed. It only varied between 14.37% recorded by neopentane and 15.73% recorded by R123. In what concerns R123, it will be phased out by 2020 according to the protocol of Montreal, which makes from cis-butene the best working fluid in our case in terms of efficiency since it recorded 15.68%. On the other hand, changing the nature of the working fluid had a significant impact on the turbine's output. Indeed, pentane allowed the turbine to produce energy as high as 85.25 kJ/kg, while this production fell down to only 36.88 kJ/kg when R245fa was selected as working fluid.

One particular parameter to be taken into consideration is the pressure of the working fluid whether it is the condensation one or the evaporation one. Four working fluids had a condensation pressure lower than the atmospheric one. This will result in a complicated and expansive condenser to avoid air infiltration. In addition, some working fluids had a high evaporation pressure like butane and cis-butene, which means an expansive evaporator will be needed in these cases.

Pentane, neopentane and isopentane released the highest amount of heat during the sub-cooling process making them good candidates for a regenerative ORC. Figure 10 presents a comparison between results obtained when using these three fluids in basic and regenerative ORCs.

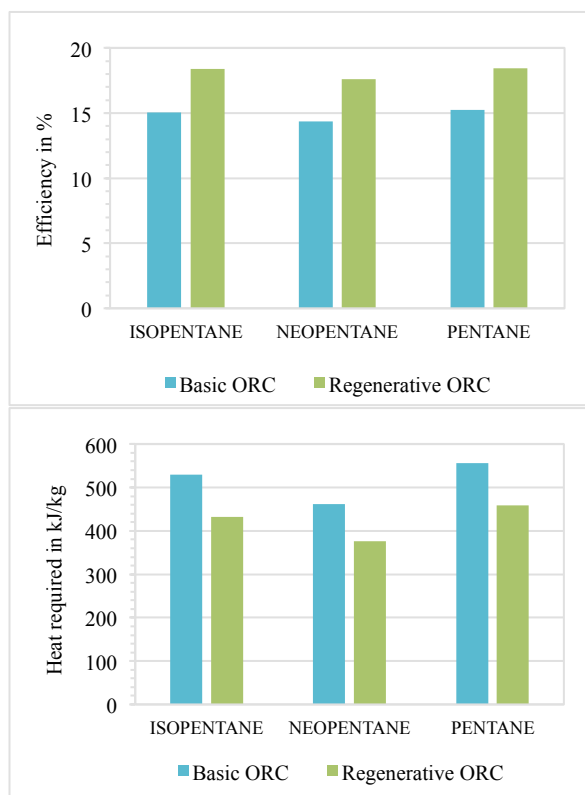


Fig. 10. Comparison of cycle efficiency and heat required during the evaporation process with basic and regenerative ORCs

Figure 10 shows that regeneration enhanced the efficiency of the three selected working fluids by 21 to 22% and their efficiencies became higher than all the other working fluids. The highest efficiency was recorded by Pentane and reached 18.46%. Moreover, regeneration made the heat required during the evaporation process lower, which is very valuable for small-scale solar applications where solar resources are limited.

3.3. The LFR-ORC power plant

Results obtained when coupling the LFR to the ORC are represented in figures from 11 to 13. The first figure shows the monthly variation of power production of cis-butene and neopentane. The other two figures give a comparison between working fluids in terms of annual power production and overall efficiency.

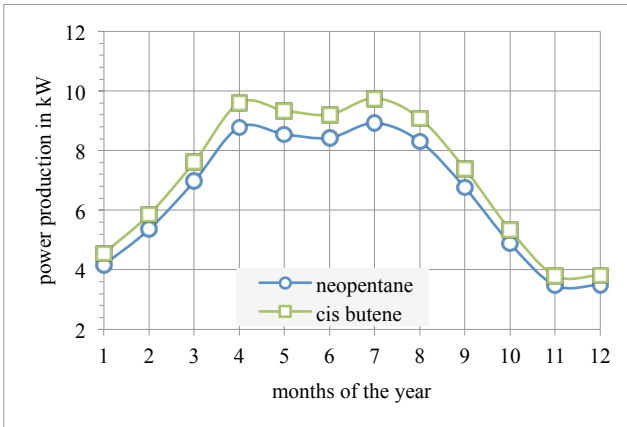


Fig. 11. monthly power production of the LFR-ORC power plant in the cases of cis-butene and neopentane

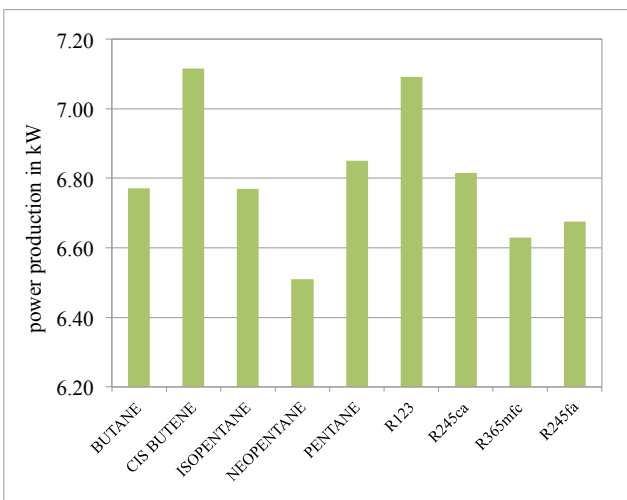


Fig. 12. Annual power production of the LFR-ORC power plant in the case of each working fluid

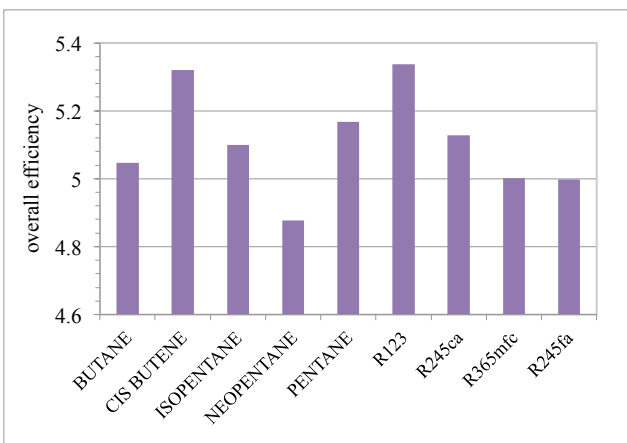


Fig. 13. Annual efficiency of the LFR-ORC power plant in case of each working fluid

Since all working fluids had the same seasonal behaviour, we only reported results obtained for cis-butene and neopentane which are the best and the worst cases consecutively. First of all, the shape of figure 11 indicates the big influence the LFR’s optical efficiency had on the power plant overall performances. In what concerns power production, it was sensibly constant from April to August

and it recorded a maximum in July and a minimum in November. For the particular case of cis-butene, the LFR-ORC power plant produced up to 9.75 kW during July and this production fell down to only 3.8 kW during November. This heavy variation is mainly derived by the variation in the LFR’s optical efficiency as it was seen in figure 7. This variation common to all working fluids makes the exploitation of such system more difficult.

Figure 12 shows that, in terms of annual power production, cis-butene and R123 was the best working fluid averaging 7.1 kW a year whereas neopentane was the worst one averaging 6.51 kW a year. In what concerns the annual efficiency of the overall system, R123 and cis-butene recorded the best annual efficiencies and it was equal to 5.32% whereas the worst working fluid was neopentane with an efficiency of 4.88% as it can be seen from figure 13.

From the previous results, one may deduce that R123 and cis-butene are the best working fluids to be used in our particular case. However, the use of R123 will be banned as of 2020. In addition, the condensation pressure of the R123 is lower than the atmospheric one unlike cis-butene. However, cis-butene has higher evaporation pressure. In what follows, we select cis-butene as the best working fluid in the case of the basic ORC configuration.

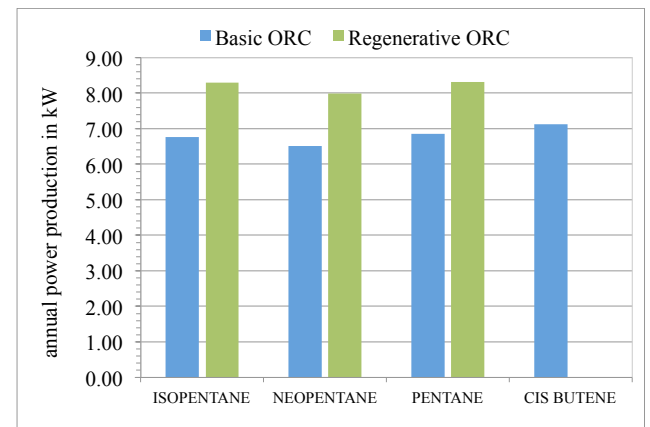


Fig. 14. Comparison between basic and regenerative ORCs in terms of annual power production

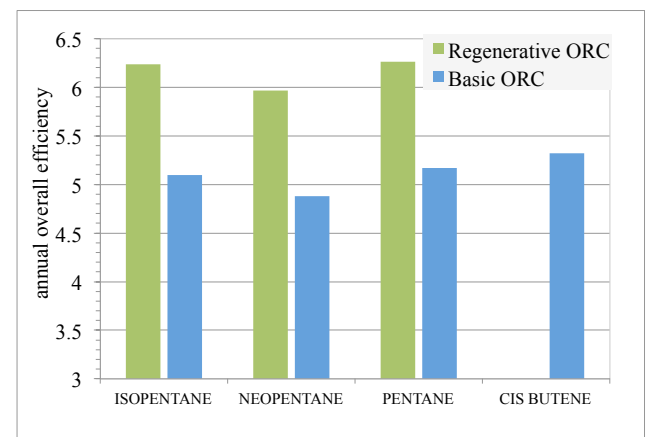


Fig. 15. Comparison between basic and regenerative ORCs in terms of annual efficiency

Figures 14 and 15 present a comparison between basic and regenerative ORCs in terms of annual power production and annual overall efficiency. It is clear from figure 14 that using regeneration enhanced the overall performances of the LFR-ORC power plant. In fact, annual power production of the three working fluids became higher than that of cis-butene, which was the best working fluid in the case of basic ORC. The same remark is true for the overall efficiency. In particular, regeneration made of pentane the best working fluid to operate the LFR-ORC power plant instead of cis-butene with an annual energy production of 8.32 kW and an overall efficiency of 6.26%. However, the condensation pressure of pentane is lower than the atmospheric pressure (only 0.68 bar). Thus, we converted to neopentane which is the only working fluid of the three selected ones who had a condensation pressure higher than the atmospheric one. Moreover, the performances of neopentane are quite close to those of pentane: its annual power production was equal to 7.99 kW and its annual overall efficiency was equal to 5.97%. Using regenerative ORC with neopentane as working fluid increased the power production of the LFR-ORC power plant by 12.22% and enhanced its overall efficiency by 12.21%.

4. Conclusion

This work investigated a small-scale LFR-ORC power plant to give preliminary insights about the feasibility of operating such systems in the region of Errachidia in Morocco. Simulations evaluated the optical performances of the LFR based solar field and the thermal performances of the power block. The main results we obtained from this work are:

- The highest monthly optical efficiency recorded by the LFR was 47.51%;
- The LFR based solar field suffered from heavy fluctuations along the year;
- The best working fluid to be used with a basic ORC was cis-butene, it recorded an annual power production of 7.12 kW and an annual overall efficiency of 5.32%;
- The best working fluid to be used with the regenerative ORC was neopentane, it recorded an annual power production of 7.99 kW and an annual optical efficiency of 5.97%;
- Using regenerative ORC increased the annual power production of the power plant by 12.22% and increased its annual overall efficiency by 12.21%.

The present work is only a preliminary assessment that we consider as a first step in our project related to the installation of a real small-scale power plant in Errachidia, Morocco. A follow up step will be the definition of the technical characteristics of each component of the system (pump, turbine, heat exchangers, piping system, ...). All of these components were only considered, in the present work, as black boxes. This step will allow us, in addition to a more realistic energetic analysed, to conduct an

economic and feasibility study of the installation given the cost of the chosen components in the local market. Moreover, the economic analysis should give answers about two major questions:

- Does the energetic gain realised by the regenerative ORC covers the cost of an additional heat exchanger (the regenerator) ?
- Which working fluid is the best one to be used given its cost and its availability ?

References

- [1] K. Rahbar, S. Mahmoud, and R. K. Al-Dadah, 'Mean-line modeling and CFD analysis of a miniature radial turbine for distributed power generation systems', *Int. J. Low-Carbon Technol.*, vol. 11, no. 2, pp. 157–168, May 2016.
- [2] H. T. Walnum, D. Rohde, and Y. Ladam, 'Off-design analysis of ORC and CO₂ power production cycles for low-temperature surplus heat recovery', *Int. J. Low-Carbon Technol.*, vol. 8, no. 1, pp. 29–36, Mar. 2013.
- [3] G. Xu, G. Song, X. Zhu, W. Gao, H. Li, and Y. Quan, 'Performance evaluation of a direct vapor generation supercritical ORC system driven by linear Fresnel reflector solar concentrator', *Appl. Therm. Eng.*, vol. 80, pp. 196–204, Apr. 2015.
- [4] S.-Y. Cho, C.-H. Cho, and Y.-B. Jung, 'Experimental Study on the Organic Rankine Cycle for Recovering Waste Thermal Energy', *Int. J. Renew. Energy Res. IJRER*, vol. 8, no. 1, pp. 120–128, Mar. 2018.
- [5] H. Ganjehsarabi, M. Asker, and A. K. Seyhan, 'Energy and exergy analyses of a solar assisted combined power and cooling cycle', in 2016 IEEE International Conference on Renewable Energy Research and Applications (ICRERA), 2016, pp. 1141–1145.
- [6] E. Georges, S. Declaye, O. Dumont, S. Quoilin, and V. Lemort, 'Design of a small-scale organic Rankine cycle engine used in a solar power plant', *Int. J. Low-Carbon Technol.*, vol. 8, no. suppl 1, pp. i34–i41, Jul. 2013.
- [7] O. Aboelwafa, S.-E. K. Fateen, A. Soliman, and I. M. Ismail, 'A review on solar Rankine cycles: Working fluids, applications, and cycle modifications', *Renew. Sustain. Energy Rev.*, vol. 82, pp. 868–885, Feb. 2018.
- [8] R. S. El-Emam and I. Dincer, 'Exergy and exergoeconomic analyses and optimization of geothermal organic Rankine cycle', *Appl. Therm. Eng.*, vol. 59, no. 1–2, pp. 435–444, Sep. 2013.
- [9] M. Uris, J. I. Linares, and E. Arenas, 'Feasibility assessment of an Organic Rankine Cycle (ORC) cogeneration plant (CHP/CCHP) fueled by biomass

- for a district network in mainland Spain', *Energy*, vol. 133, pp. 969–985, Aug. 2017.
- [10] K. Qiu and E. Thorsteinson, 'An organic Rankine cycle system for solar thermal power applications', in *2014 International Conference on Renewable Energy Research and Application (ICRERA)*, 2014, pp. 138–141.
- M. H. Ahmed, M. Rady, A. M. A. Amin, F. M. Montagnino, and F. Paredes, 'Comparison of thermal and optical performance of Linear Fresnel and Parabolic Trough Concentrator', in *2015 International Conference on Renewable Energy Research and Applications (ICRERA)*, 2015, pp. 626–629.
- [11] Y. İ. Tosun, '5MW hybrid power generation with agriculture and forestry biomass waste co-incineration in stoker and subsequent solar panel (CSP) ORC station', in *2015 International Conference on Renewable Energy Research and Applications (ICRERA)*, 2015, pp. 583–589.
- [12] G. Cau and D. Cocco, 'Comparison of Medium-size Concentrating Solar Power Plants based on Parabolic Trough and Linear Fresnel Collectors', *Energy Procedia*, vol. 45, pp. 101–110, 2014.
- [13] N. B. Desai and S. Bandyopadhyay, 'Thermo-economic analysis and selection of working fluid for solar organic Rankine cycle', *Appl. Therm. Eng.*, vol. 95, pp. 471–481, Feb. 2016.
- [14] L. Cioccolanti, R. Tascioni, and A. Arteconi, 'Simulation analysis of an innovative micro-solar 2kWe Organic Rankine Cycle plant for residential applications', *Energy Procedia*, vol. 142, pp. 1629–1634, Dec. 2017.
- [15] D. Cocco and F. Serra, 'Performance comparison of two-tank direct and thermocline thermal energy storage systems for 1 MWe class concentrating solar power plants', *Energy*, vol. 81, pp. 526–536, Mar. 2015.
- [16] S. Rodat, R. Bavière, A. Bruch, and A. Camus, 'Dynamic simulation of a Fresnel solar power plant prototype with thermocline thermal energy storage', *Appl. Therm. Eng.*, vol. 135, pp. 483–492, May 2018.
- [17] M. Cagnoli, D. Mazzei, M. Procopio, V. Russo, L. Savoldi, and R. Zanino, 'Analysis of the performance of linear Fresnel collectors: Encapsulated vs. evacuated tubes', *Sol. Energy*, vol. 164, pp. 119–138, Apr. 2018.
- [18] F. A. Boyaghchi and A. Sohatloo, 'Assessment and optimization of a novel solar driven natural gas liquefaction based on cascade ORC integrated with linear Fresnel collectors', *Energy Convers. Manag.*, vol. 162, pp. 77–89, Apr. 2018.
- [19] M. Petrollese, D. Cocco, and G. Cau, 'Small-scale CSP plant coupled with an ORC system for providing dispatchable power: the Ottana Solar Facility', *Energy Procedia*, vol. 129, pp. 708–715, Sep. 2017.
- [20] D. Cocco, V. Tola, and M. Petrollese, 'Application of Concentrating Solar Technologies in the Dairy Sector for the Combined Production of Heat and Power', *Energy Procedia*, vol. 101, pp. 1159–1166, Nov. 2016.
- [21] P. Tsekouras, C. Tzivanidis, and K. Antonopoulos, 'Optical and thermal investigation of a linear Fresnel collector with trapezoidal cavity receiver', *Appl. Therm. Eng.*, vol. 135, pp. 379–388, May 2018.
- [22] 'SolTrace | Concentrating Solar Power | NREL'. [Online]. Available: <https://www.nrel.gov/csp/soltrace.html>. [Accessed: 11-Oct-2018].
- [23] 'HelioClim-3 Archives for Free - www.soda-pro.com'. [Online]. Available: <http://www.soda-pro.com/web-services/radiation/helioclim-3-archives-for-free>. [Accessed: 14-May-2018].
- [24] S. G. Johnson, 'REFPROP', NIST, 18-Apr-2013. [Online]. Available: <https://www.nist.gov/srd/refprop>. [Accessed: 14-May-2018].
- [25] E. Ghasemian and M. A. Ehyaei, 'Evaluation and optimization of organic Rankine cycle (ORC) with algorithms NSGA-II, MOPSO, and MOEA for eight coolant fluids', *Int. J. Energy Environ. Eng.*, vol. 9, no. 1, pp. 39–57, Mar. 2018.
- [26] Y. Qiu, Y.-L. He, Z.-D. Cheng, and K. Wang, 'Study on optical and thermal performance of a linear Fresnel solar reflector using molten salt as HTF with MCRT and FVM methods', *Appl. Energy*, vol. 146, pp. 162–173, May 2015.
- [27] Y. Elmaanaoui and D. Saifaoui, 'Parametric analysis of end loss efficiency in linear Fresnel reflector', in *2014 International Renewable and Sustainable Energy Conference (IRSEC)*, 2014, pp. 104–107.